

NASA/GSFC

Memorandum

To: IXO Project Managers
From: A. Ptak
Date: June 25, 2010
Re: IXO response matrices

Ref: IXO-TM-001150

Introduction

This memo is intended to document the IXO responses matrices created in May/June, 2010. The focal plane instrument teams produced descriptions of the detector efficiencies along with tables giving the net efficiency as a function of energy, in some cases additionally for the cases of several filter wheel settings. These efficiency curves were then combined with the Silicon Pore optics (SPO) Flight Mirror Assembly (FMA) effective area (EA) to create SPO responses, with both the mirror area calculation and response file generation performed by Tim Oosterbroek (see IXO_Matrices_v2.0.pdf, SRE-PA/2010.037/v2.0, IXO GSFC library IXO-MEMO-001147). As discussed below, the same instrument responses were used in combination with segmented glass FMA EA calculations performed by Paul Reid (given in EA_012109 fma design_051010pbr_mirror-xms-xgs-wfi.xls, with methodology detailed in IXO-MEMO-001076) to generate glass response matrices (produced by Andy Ptak). In both cases the mirror EA curves include obscuration by the CAT-XGS grating and the grating zero-order. The SPO EA assumes a constant 10% loss factor (due to alignment error and particulate contamination), while the glass mirror includes a net loss factor varying from 4% at 0.1 keV to 8% at 12 keV. The glass EA loss factor is comprised of a 4% loss (energy-independent) due to alignment errors and particulate contamination, an energy-dependent scattering factor and a 300 Å thermal shield covering the inner modules. Note that the glass EA does not include the hard X-ray mirror module (HXMM).

The XGS effective areas were calculated as described in CATXGS_effective_area_2010_04_21.xls and OPXGS_Aeff_Tech_note_V2.pdf for the case of the critical angle transmission (CAT) grating and the off-plane (OP) grating coupled with the SPO optics. Details concerning the grating effective area computation for the glass optics will be given in a later version of this document.

Response Generation

All glass response files were generated by the fool rspgen which produces a single rsp file containing a matrix extension with the redistribution from energy space to channel space and the effective area. At a later date separate rmf and arfs will be created, i.e., with a single rmf for a given detector for use with both the SPO and glass FMA designs. rspgen takes as input the mirror effective area and detector efficiency files or a single

effective area file. The spectral line response function is a single Gaussian with the same energy resolution as a function of energy as was used in creating the SPO responses (see Table 1 and IXO_Matrices_v2.0.pdf). Note that the FWHM-energy function for the XGS is artificial in the sense that it simply assumes $R=3000$ (the requirement), while in practice individual orders will be combined in some sense resulting in a more complicated FWHM energy dependence. The energy and channel space binning was also chosen to match the corresponding SPO matrices, which was linear except for the XMS response.

For each response, plots were generated showing the effective area (i.e., rsp row sum versus energy), derived full-width half-maximum (FWHM) line response width, and “binning” = FWHM / channel binning. The derived FWHM was computed by taking the peak value in each rsp row and determining the channels at which $\frac{1}{2}$ of the max. is reached (using interpolation to mitigate coarse binning in some cases). The FWHM plot shows the derived FWHM along with the input FWHM relation. Note that the “measured” FWHM is only calculated for rsp rows with a total effective area $> 1 \text{ cm}^2$ since the FWHM becomes undefined as the area goes to 0. As a result FWHM = 0 for most focal plane instruments above 10 keV, with the SPO design resulting in more area above 10 keV (and hence more rows with $EA > 1 \text{ cm}^2$). The binning plot uses the assumed (not measured) FWHM and gives an indication of how well the line response function is being sampled.

Instrument	FWHM (keV)
XMS	$0.0025 \text{ E}^{<7.}; \text{E}/2800. \text{ E}^{>7.}$
WFI	$\sqrt{2315.9 \cdot \text{E} + 657.714} / 1000.$
HTRS	$0.001 \cdot [84.3111 - 25.018 \cdot \text{E} + 0.06987(\text{E} \cdot 1000)^{0.919449}]$
HXI	$0.001 \cdot [350. + \sqrt{2 \cdot \text{E} \cdot 1000.}]$
XGS	$\text{E}/3000.$
X-POL	$0.2 \cdot \text{E} \cdot \sqrt{6./\text{E}}$

Table 1: FWHM dependence on energy, taken from IXO_Matrices_v2.0.pdf. E in keV.

The total effective area and “net” efficiency is shown for each detector/filter + mirror design pair of responses. The net efficiency is defined as the total effective area in the response divided by the mirror effective area shown in Figure 1. The input efficiency (discussed in IXO_Matrices_v2.0.pdf and uploaded to <http://ixo.cfa.harvard.edu/wiki/IXO/Resources/IXOSimResponse>) is also plotted. These curves should agree perfectly and only differ due to interpolation and numerical errors. The efficiency calculated based on the parameters given in the corresponding instrumental efficiency reports (see the Appendix for details) is also shown. In general these efficiency curves agree with each other. The main discrepancies are “glitches” in the glass efficiency re-derived from the final rsp and the input mirror area (red curves) and differences in low-energy end of the manually-computed efficiencies (black dashed curves, discussed in the Appendix). In both cases sampling near sharp response features (e.g., absorption edges) seems to be the main issue.

Effective Area

The effective area at the focal plane (i.e., including CAT-XGS obscuration and zero-order) based on current designs are shown in Figure 1.

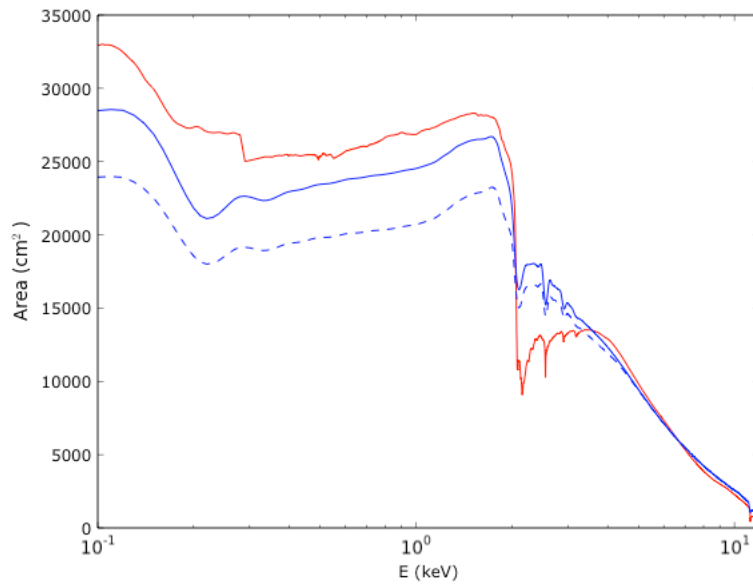


Figure 1: Focal-plane Effective Area for Glass (red), SPO, baseline design (blue) and SPO, 2.5 m² minimum design (blue dashed)

XMS

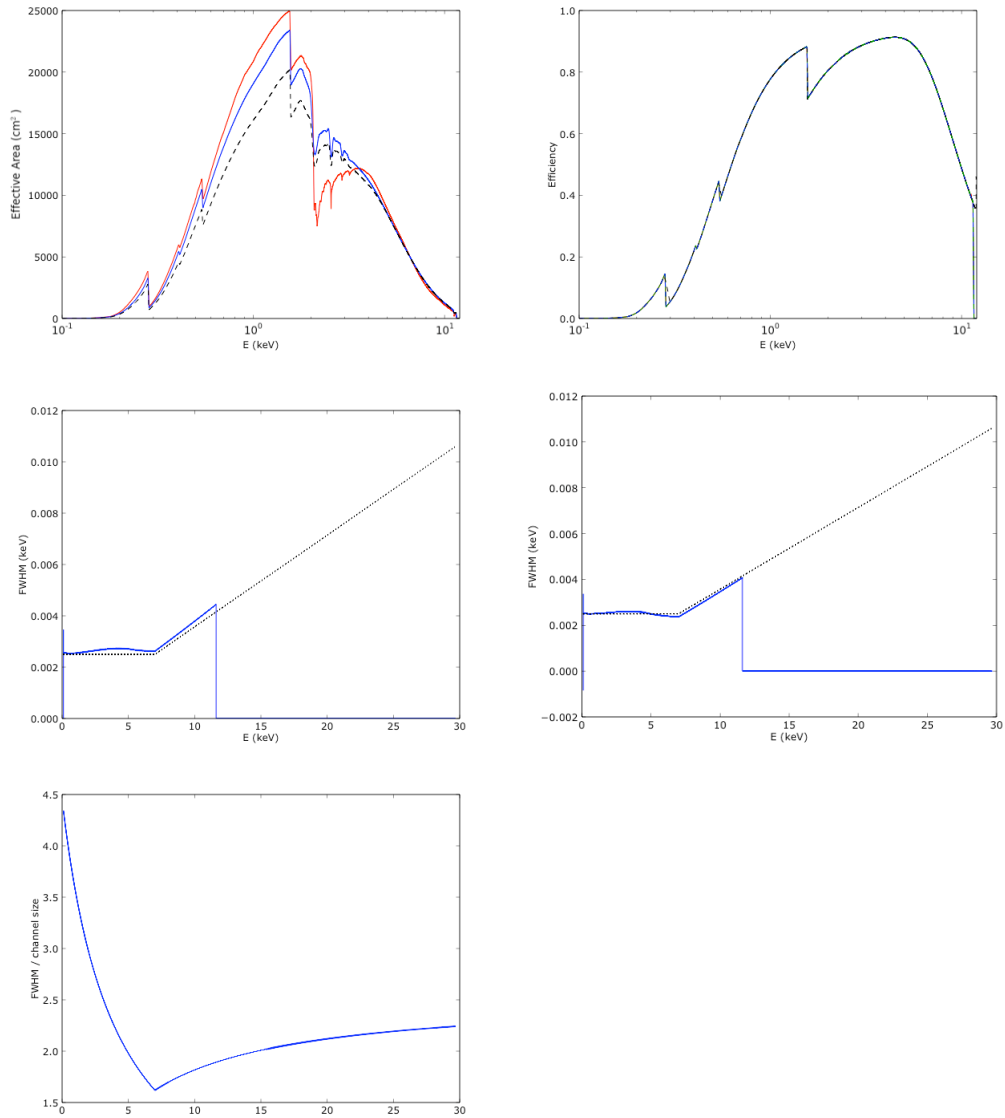


Figure 2: (top left) XMS total effective area for the glass (red), SPO baseline (blue), and SPO minimum (blue dashed) designs. (top right) Detector efficiency inferred from glass response file (red), SPO baseline (blue), SPO minimum (blue dashed), the detector efficiency file (green dashed) and calculated as discussed in the Appendix (black dashed). (middle) (spectral) FWHM derived from glass (left) and SPO (right) response file (blue) and input FWHM (black dotted). (bottom) FWHM / spectral bin size

WFI

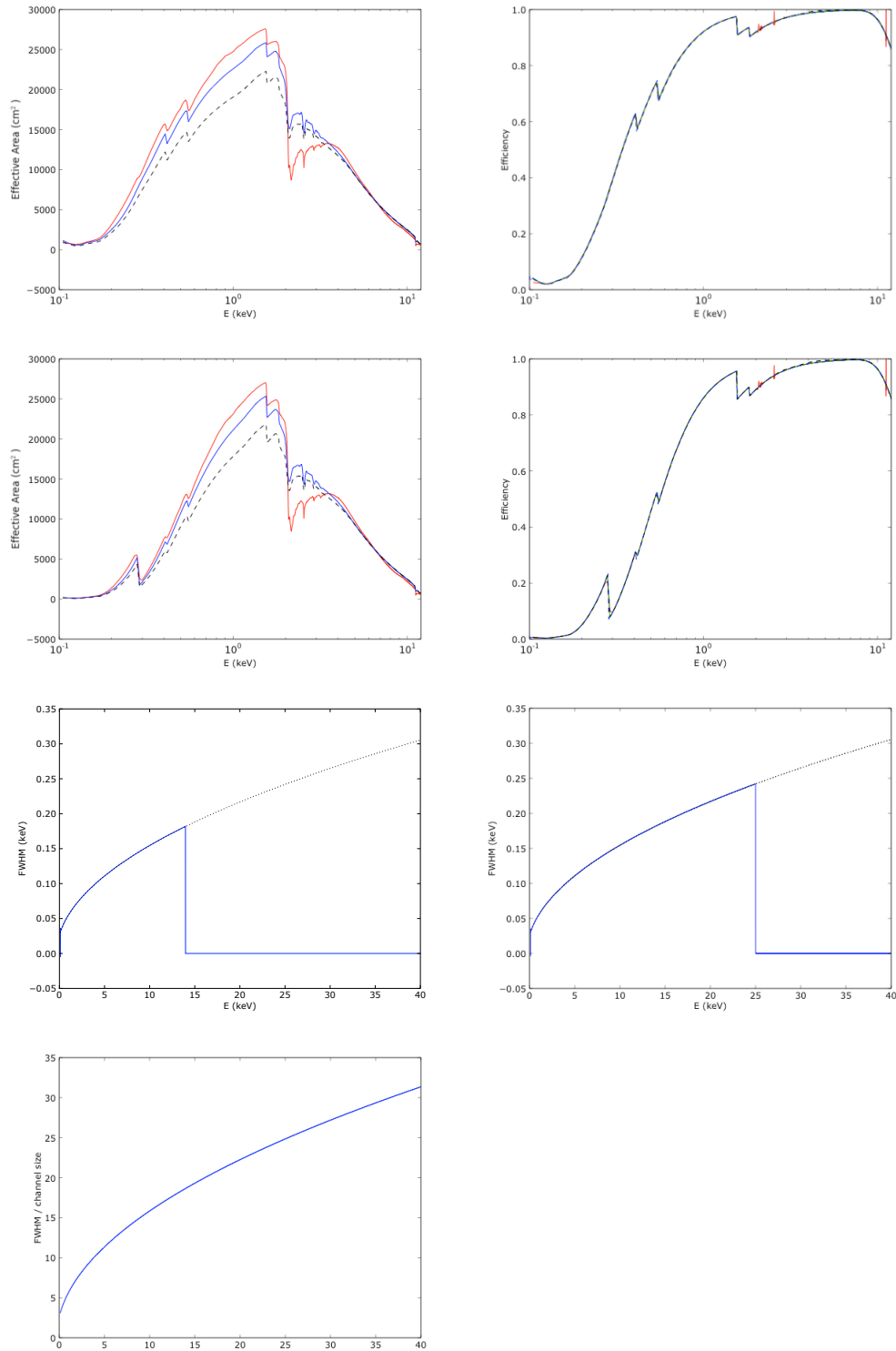


Figure 3: As in Figure 2 except top 2 rows show the open and Al+PP filter configurations.

CAT-XGS

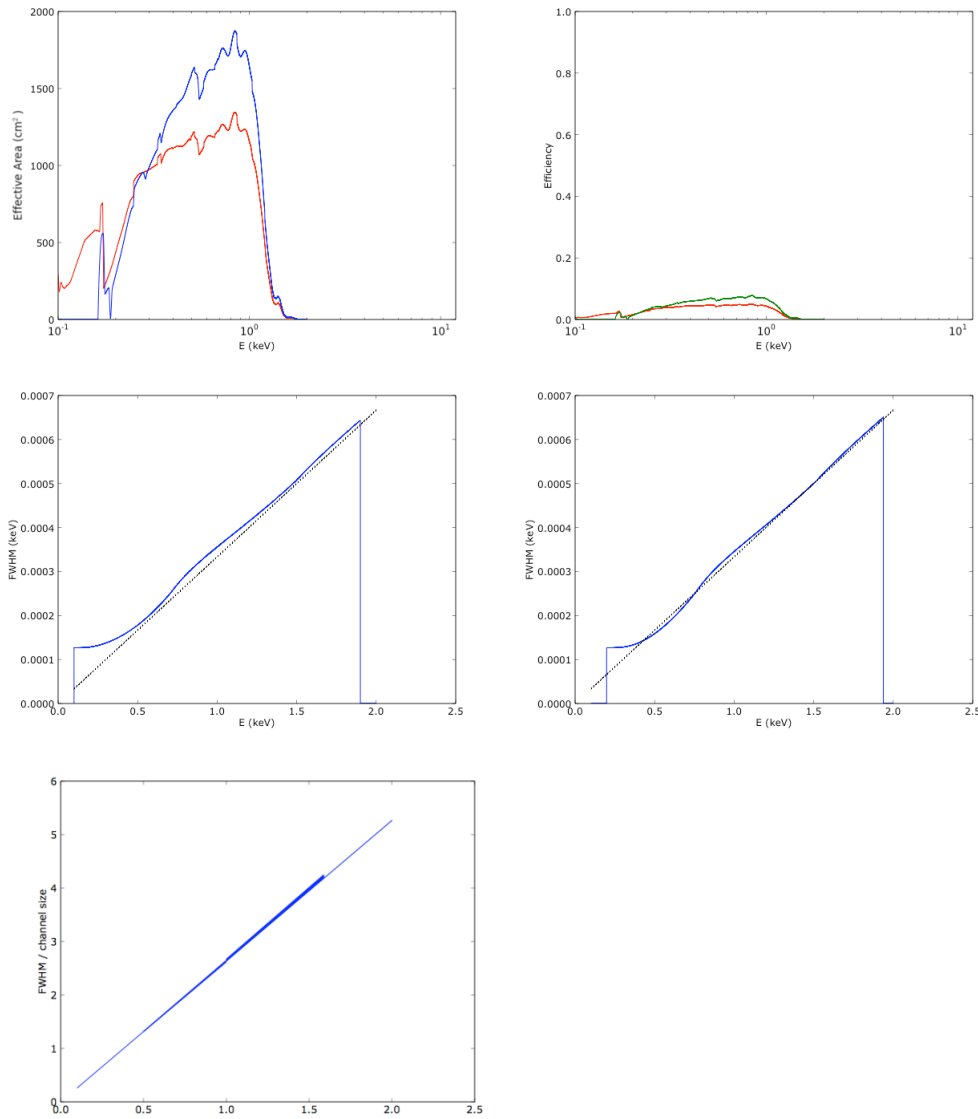


Figure 4: As in Figure 2 except for the CAT-XGS. Note that the “efficiency” plot is not meaningful in the same way as for the focal plane instruments since the focal plane mirror area, which was divided from the rsp area, was not used in computing the response. Therefore the plot is just shown to give a crude estimate of the fraction of light that is detected in the grating ccds relative to the focal plane instruments.

OP-XGS

The OP-XGS response for the SPO mirror design has been calculated and the diagnostics plots are shown here. The OP-XGS response for the glass FMA is being computed and the glass/spo comparison plots will be added when available.

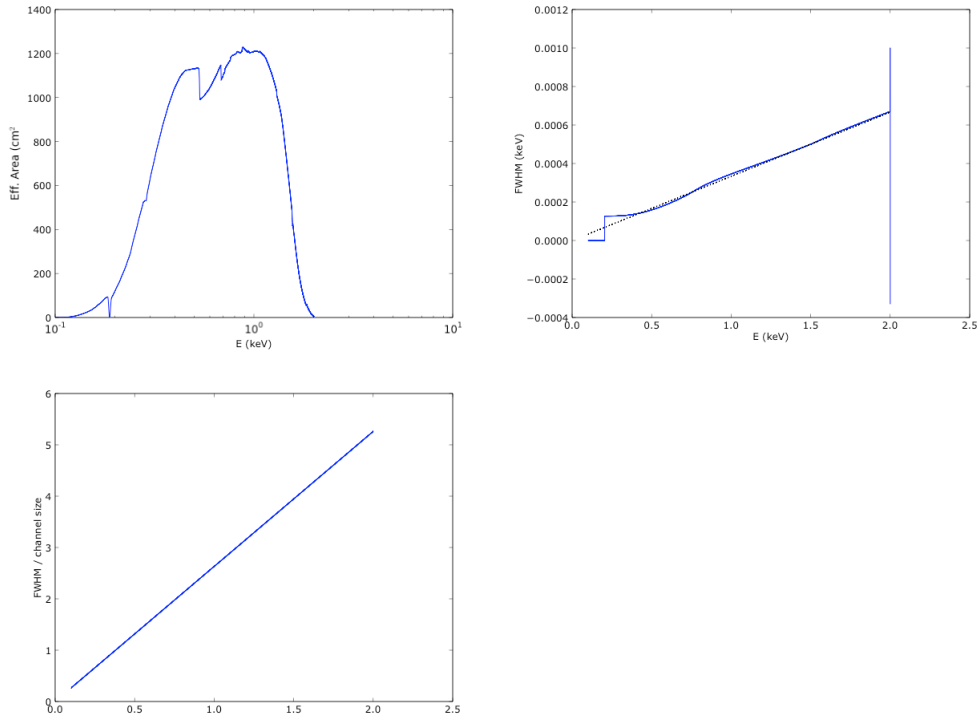


Figure 5: Total area (top left), FWHM (top right) and binning (bottom) for the SPO OP-XGS.

HTRS

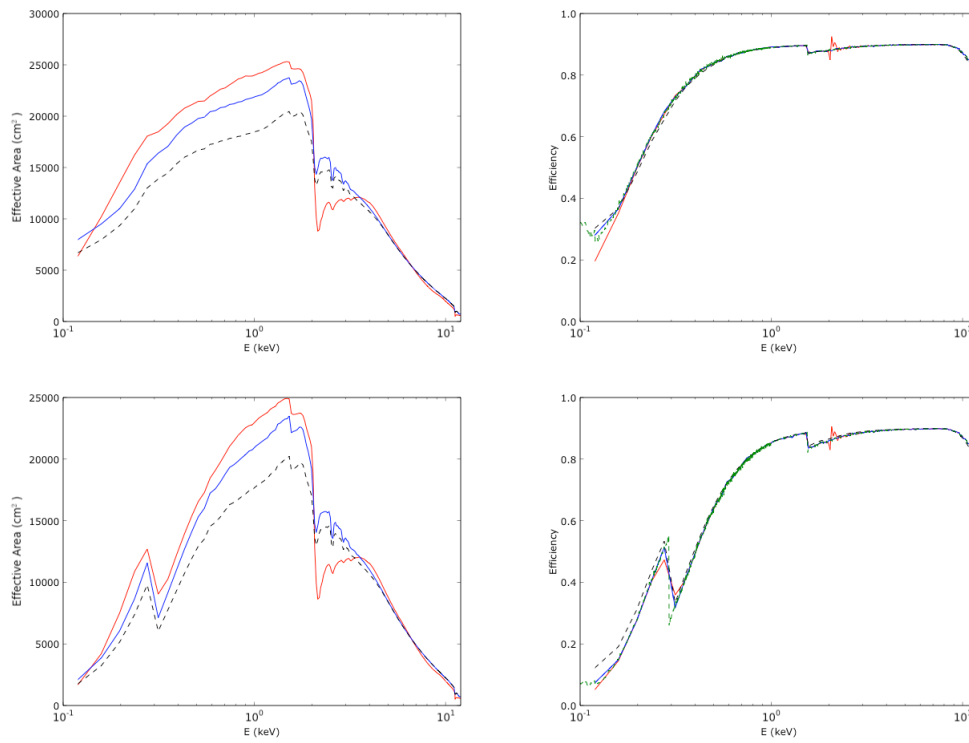


Figure 6a: The HTRS effective area and efficiency for the open (top) and thin (bottom) filters.

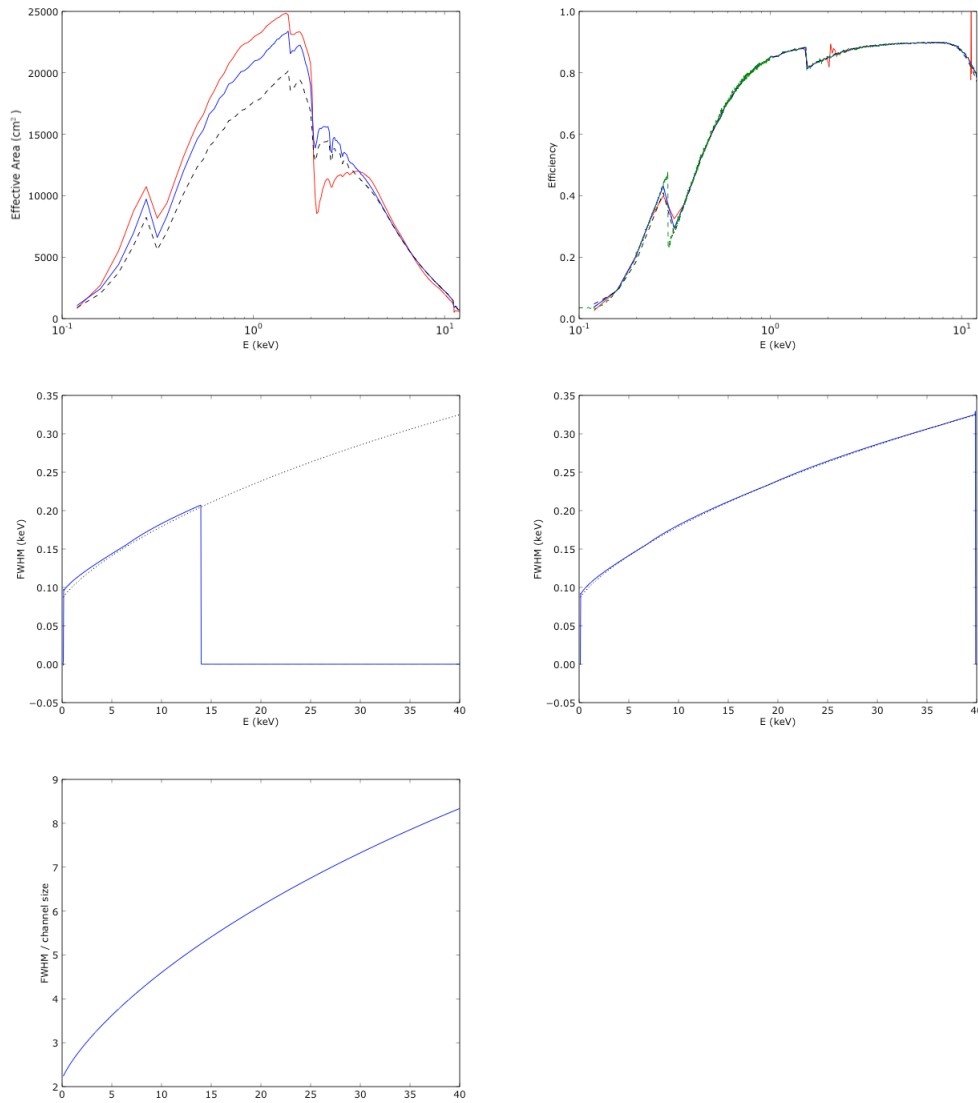


Figure 6b: As in Figure 2 except for the HTRS thick filter. The FWHM and binning plots are of course independent of the filter configuration.

X-POL

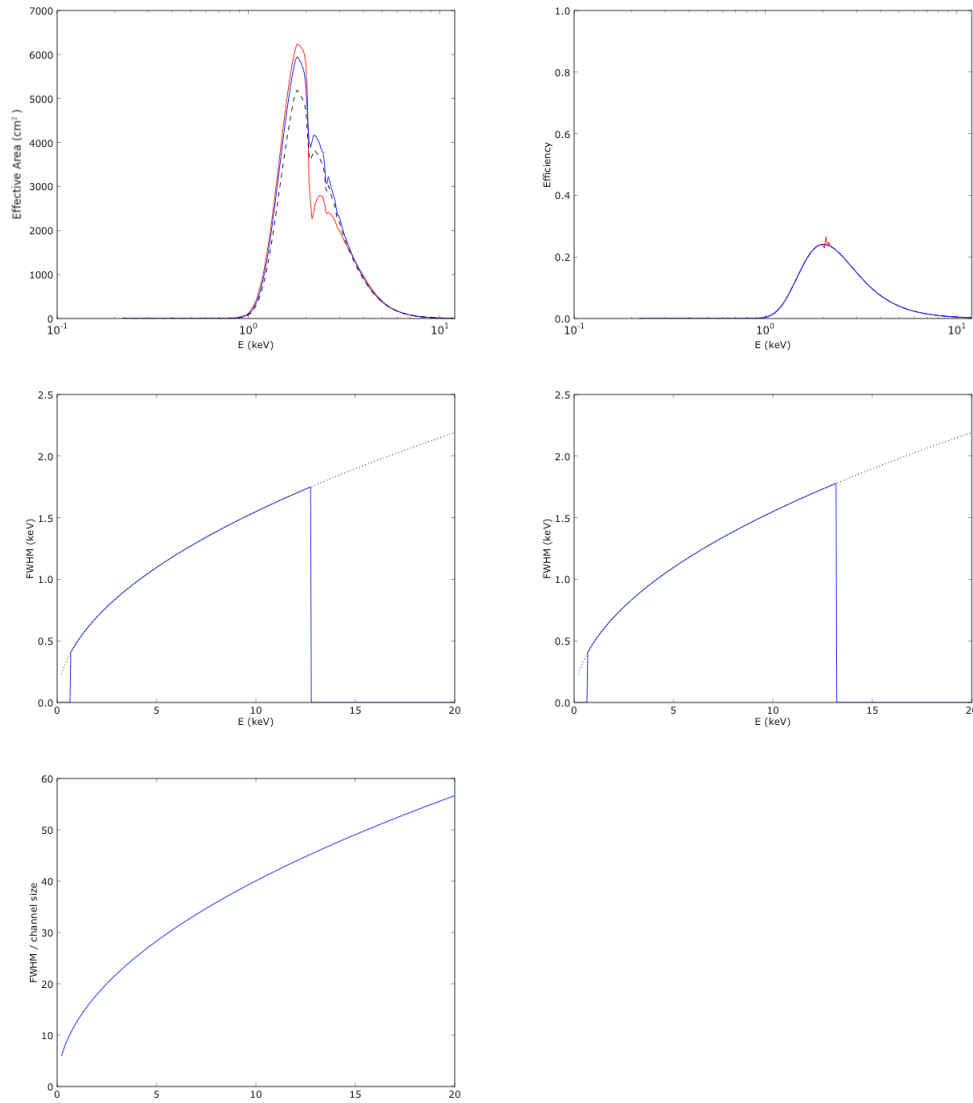


Figure 7: As in figure 2 except for the X-POL.

HXI

Only a single HXI response is available at the moment. This response is based on the SPO design and assumes (from T. Oosterbroek): Japanese reflectivity tables for the innermost modules (R within ~ 45 cm), plus a small contribution from the B4C coated mirror modules at the lower part of the HXI band. The area is calculated from 0.1 to 80 keV based on B4C reflectivities outside $r \sim 45$ cm and Japanese ML reflectivities inside $r \sim 45$ cm.

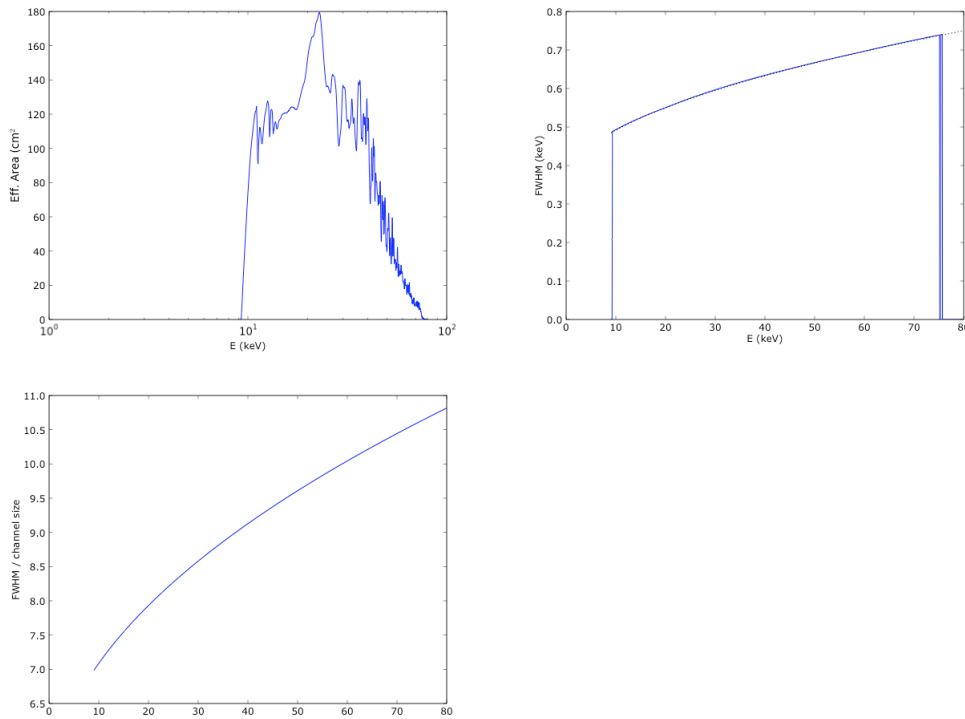


Figure 8: The total EA (top left), FWHM (top right) and binning (bottom) are shown.

Appendix

Detector efficiencies (other than the gratings) are calculated based on the absorption in the bulk material and transmission through the filters and any other obstructing material, e.g., molecular contamination, plotted as dashed black lines in the response efficiency plots. Here the calculations are performed with the python script `calc_QE.py` posted on the IXO wiki. The relevant equations are:

$$QE = F_{fill}(1 - F_{dead}) \exp\left(-\sum_i \tau_{filter,i}\right) \left(1 - \exp\left[-\sum_j \tau_{bulk,i}\right]\right)$$

where F_{fill} = the fill fraction, F_{dead} = dead area fraction, and τ_{filter} and τ_{bulk} are the filter (again more generally any material along the line of sight to the detector) and bulk optical depths. τ_{filter} and τ_{bulk} are calculated based on optical data at

http://henke.lbl.gov/optical_constants. In the case of solid molecular materials, the filter transmission tool is used (http://henke.lbl.gov/optical_constants/filter2.html, where the default densities at that site are assumed) while gas transmission was calculated using http://henke.lbl.gov/optical_constants/gastrn2.html. For atomic data the imaginary part of the atomic scattering factor (f_2) was used as follows:

$$\tau = \frac{2r_e \lambda f_2 \rho N_A d}{W}$$

where r_e is the classical electron radius, λ is the photon wavelength, ρ is the mass density, N_A is Avogadro's Number, W is the atomic weight and d is the material thickness.

The table below gives the assume filter and bulk thicknesses. Note that in the case of the X-POL, the bulk absorber is gas and the "thickness" parameters approximate a mixture of the He and dimethyl ether (DME).

Detector	Dead Fraction	Fill Fraction	Filter		Bulk	
			Name	d (nm)	Name	d
XMS	0.02	0.95	Polyimide	280	Au	1.0 μm
			Al	210	Bi	4.0 μm
			C*	2		
			H ₂ O*	6		
WFI	0.0	1.00	Si	6	Si	450. μm
			Al	70		
			SiO ₂	50		
			Si ₃ N ₄	30		
			Al	40		
			C ₃ H ₆	320		
HTRS	0.1	1.00	Si	6	Si	450. μm
			Al	30		
			Al	20		
			C ₃ H ₆	200		
			Al	50		
			C ₃ H ₆	200		
X-POL (gas at 800 torr)	0.00	1.00			He	2 mm
					DME	8 mm

* Beginning-of-life contamination

Energy Conversion Factors

Energy conversion factors (ECFs) are the conversion from flux to count rate for a given model (ECF = count rate / flux). Here we give ECFs for the responses matrices discussed above computed for a simple power-law model with $\Gamma=1.8$ and $N_H=5 \times 10^{20} \text{ cm}^{-2}$ and are scaled by $10^{-13} \text{ ergs s}^{-1} \text{ cm}^{-2}$. Most of the ECFs are ~ 1 in the 0.5-10.0 keV band, so typical IXO count rates for an $F_X \sim 10^{-13} \text{ ergs s}^{-1} \text{ cm}^{-2}$ source should be ~ 1 cts/s.

Response File	Energy Range	ECF x 10^{-13}
ixo_glass_xms_none_20100524	0.5-2.0	1.1
ixo_glass_xms_none_20100524	2.0-10.0	0.14
ixo_spo_xms_none_20100527	0.5-2.0	1.0
ixo_spo_xms_none_20100527	2.0-10.0	0.16
ixo_spo_xms_none_2.5_20100527	0.5-2.0	0.88
ixo_spo_xms_none_2.5_20100527	2.0-10.0	0.15
ixo_glass_catxgs_none_20100524	0.5-2.0	0.053
ixo_spo_catxgs_none_20100519	0.5-2.0	0.073
ixo_spo_opxgs_none_20100519	0.5-2.0	0.061
ixo_glass_htrs_open_20100524	0.5-2.0	1.4
ixo_glass_htrs_open_20100524	2.0-10.0	0.14
ixo_spo_htrs_open_20100527	0.5-2.0	1.3
ixo_spo_htrs_open_20100527	2.0-10.0	0.16
ixo_spo_htrs_open_2.5_20100527	0.5-2.0	1.1
ixo_spo_htrs_open_2.5_20100527	2.0-10.0	0.16
ixo_glass_htrs_thick_20100524	0.5-2.0	1.3
ixo_glass_htrs_thick_20100524	2.0-10.0	0.14
ixo_spo_htrs_thick_20100527	0.5-2.0	1.2
ixo_spo_htrs_thick_20100527	2.0-10.0	0.16
ixo_spo_htrs_thick_2.5_20100527	0.5-2.0	0.99
ixo_spo_htrs_thick_2.5_20100527	2.0-10.0	0.15
ixo_glass_htrs_thin_20100524	0.5-2.0	1.3
ixo_glass_htrs_thin_20100524	2.0-10.0	0.14
ixo_spo_htrs_thin_20100527	0.5-2.0	1.2
ixo_spo_htrs_thin_20100527	2.0-10.0	0.16
ixo_spo_htrs_thin_2.5_20100527	0.5-2.0	1.0
ixo_spo_htrs_thin_2.5_20100527	2.0-10.0	0.15
ixo_glass_xpol_20100524	0.5-2.0	0.070
ixo_glass_xpol_20100524	2.0-10.0	0.024
ixo_spo_xpol_default_20100527	0.5-2.0	0.067
ixo_spo_xpol_default_20100527	2.0-10.0	0.028
ixo_spo_xpol_default_2.5_20100527	0.5-2.0	0.058
ixo_spo_xpol_default_2.5_20100527	2.0-10.0	0.026
ixo_glass_wfi_open_20100625	0.5-2.0	1.4
ixo_glass_wfi_open_20100625	2.0-10.0	0.16

ixo_spo_wfi_open_20100527	0.5-2.0	1.3
ixo_spo_wfi_open_20100527	2.0-10.0	0.18
ixo_spo_wfi_open_2.5_20100527	0.5-2.0	1.1
ixo_spo_wfi_open_2.5_20100527	2.0-10.0	0.17
ixo_glass_wfi_Al+PP_20100625	0.5-2.0	1.3
ixo_glass_wfi_Al+PP_20100625	2.0-10.0	0.15
ixo_spo_wfi_Al+PP_20100527	0.5-2.0	1.2
ixo_spo_wfi_Al+PP_20100527	2.0-10.0	0.18
ixo_spo_wfi_Al+PP_2.5_20100527	0.5-2.0	0.99
ixo_spo_wfi_Al+PP_2.5_20100527	2.0-10.0	0.17
ixo_spo_hxi_none_20100527	10.0-30.0	0.00046
ixo_spo_hxi_none_2.5_20100527	10.0-30.0	0.00047